Electronic Supplementary Material (ESI) for ChemComm.
This journal is © The Royal Society of Chemistry 2022

Supporting Information

Thermal Enhancement of Upconversion in Lanthanide-doped $Gd_2Ti_2O_7$ Crystals via fast evaporation in sol-gel procedure

Yi Cheng,[a] Yubin Wang[a] Denghao Li,[a] Juan Bao,[a] Degang Deng,[a] Hai Guo,*[b] Lei Lei*[a]

[a] *Key Laboratory of Rare Earth Optoelectronic Materials and Devices of Zhejiang Province,* College of Optical and Electronic technology, China Jiliang University, Hangzhou 310018, China

[b] *Department of Physics, Zhejiang Normal University, Jinhua, Zhejiang 321004, China*

EXPERIMENTAL SECTION

Chemicals and Reagents. NH_4F (98%),NaOH(⩾96%), $Gd(Ac)_3 \cdot xH_2O$ (99.9%), $Tm(Ac)_3 \cdot xH_2O$ (99.9%), $Yb(Ac)_3 \cdot xH_2O$ (99.9%), 1-Octadecene (ODE, 90%) and Oleic acid (OA, 90%) were supplied by Sigma Aldrich Company. $Yb(NO_3)_3 \cdot xH_2O$ (99.9%), $Er(NO_3)_3 \cdot xH_2O$ (99.9%), $Gd(NO_3)_3 \cdot xH_2O$ (99.9%), $C_{16}H_{36}O_4Ti$, citric acid, cyclohexane, methanol and absolute ethanol were purchased from Sinopharm Chemical Reagent Company. All chemicals were of analytical grade and used as received without further purification.

Synthesis of $NaGdF_4$: 49Yb/1Tm NCs. $Gd(Ac)_3$ (0.5 mmol), $Yb(Ac)_3$ (0.49 mmol) and $Tm(Ac)_3$ (0.01 mmol) ware added into a 50 mL three-necked bottle containing 10 mL OA. The mixture was heated at 150 °C for 30 min to remove water from the solution. Then 15 mL ODE was quickly added to the above solution and the resulted

mixture was heated at 150 °C for another 30 min to form a clear solution, and then cooled down to room temperature. Afterwards, 8 mL methanol solution containing NH_4F (3.75 mmol) and NaOH (2.5 mmol) were added into the above solution and stirred at 60 °C for 30 min. After the methanol was evaporated, the solution was further heated to 290 °C under N_2 atmosphere and kept for 90 min, and then cooled down to room temperature. The products were precipitated by addition of ethanol, collected by centrifugation, washed with ethanol for three times, and finally re-dispersed in 4 mL cyclohexane.

Synthesis of $NaGdF_4$: 49Yb/1Tm@$NaYF_4$ core-shell NCs. $Y(Ac)_3$ (1 mmol) was added into a 50 mL three-necked bottle containing OA (10 mL). The mixture was heated at 150 °C for 30 min to remove water from the solution. A solution of ODE (15 mL) was then quickly added and the resulted mixture was heated at 150 °C for another 30 min to form a clear solution, and then cooled down to 80 °C. Thereafter, the pre-prepared $NaGdF_4$: 49Yb/1Tm core NCs in 4 mL cyclohexane was added to the above solution and kept at 110°C for 40 min. After the removal of cyclohexane, 8 mL methanol solution containing NH_4F (3.75 mmol) and NaOH (2.5 mmol) were added and the solution was stirred at 60 °C for 30 min. After the methanol was evaporated, the solution was further heated at 290 °C under N_2 for 120 min, and finally cooled down to room temperature.

Synthesis of Er^{3+}, Ho^{3+}, doped $Gd_2Ti_2O_7$ NCs. Taking $Gd_2Ti_2O_7$: 30Yb/4Er as an example, Add $Gd(NO_3)_3 \cdot xH_2O$ (1.32mmol), $Yb(NO_3)_3 \cdot xH_2O$ (0.6mmol) and $Er(NO_3)_3 \cdot xH_2O$ (0.08mml) into 8ml ethanol, mix and stir for 10 minutes, add citric acid (4mmol) and continue stirring for 30 minutes, add tetrabutyl titanate (2.5mm) and continue stirring for 30 minutes, then heat and dry at 140 °C, grind

the obtained product into powder, place it in a crucible in an oven and sinter at 1000 °C for 5 hours. In the control experiment, the amount of ethanol was 4ml and 16ml, and the drying temperature was 60 °C and 100 °C.

Characterizations. X-ray diffraction (XRD) analysis was carried out with a powder diffractometer (Bruker D8 Advance) with a Cu-Kα (λ=1.5405 Å) radiation. The morphology and scanning transmission electron microscopy (STEM) of the products were characterized by a field emission transmission electron microscopy (TEM, FEI Tecnai G2 F20) equipped with an energy dispersive X-ray spectroscope (EDS, Aztec X-Max 80T). UC emission spectra and life-time were carried out on an Edinburgh Instruments FLS920 spectrofluorometer equipped with an adjustable laser diode (980 nm). The 980 nm laser for illuminating photographs is connected with a beam expander to obtain a big beam size of about 2.5 cm in diameter.

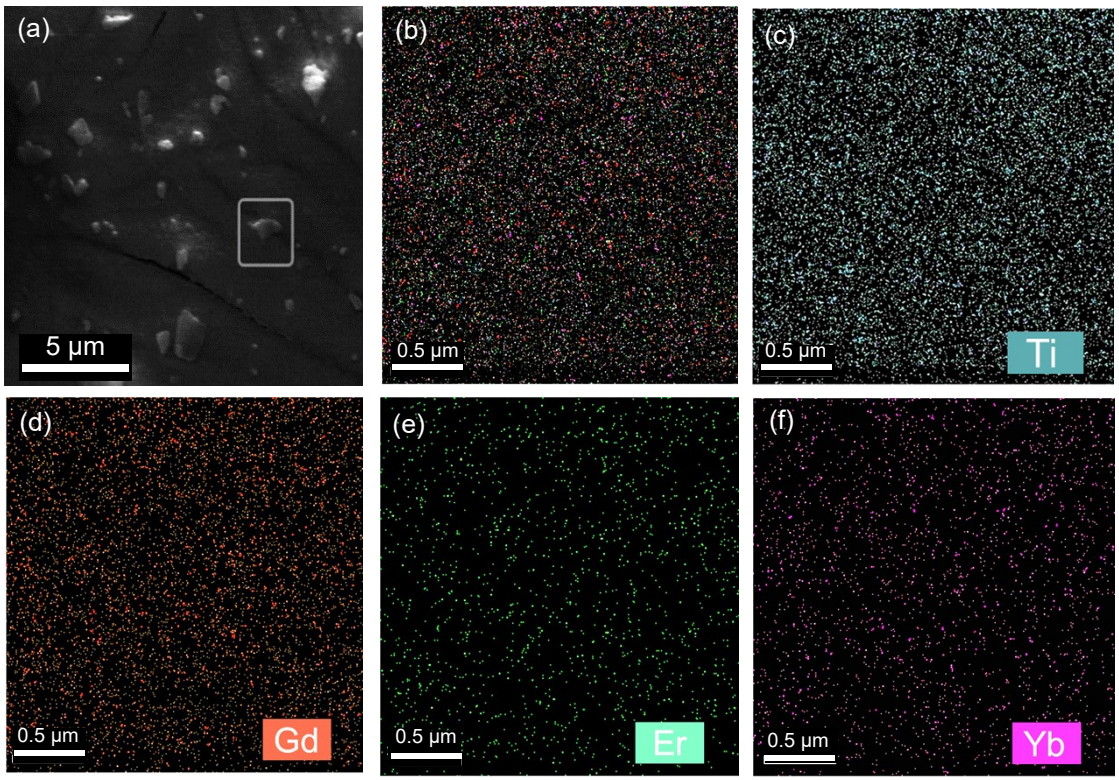

Figure S1. EDX mappings of mixed (b),Ti (c), Gd (d), Er (e), and Yb (f) elements of the $Gd_2Ti_2O_7$: 30Yb/4Er NCs (a).

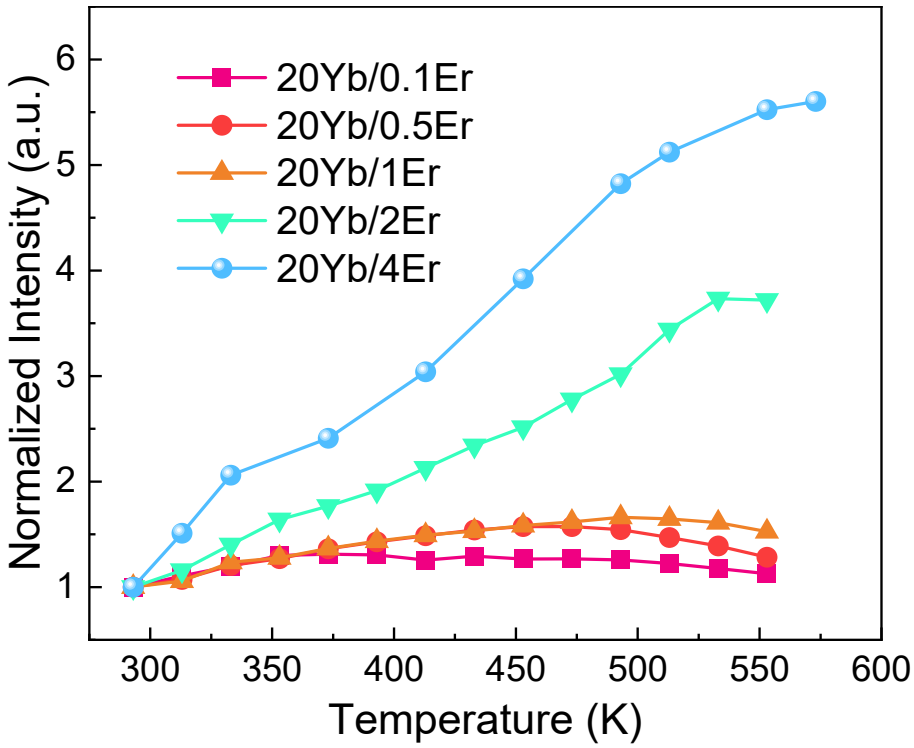

Figure S2. The normalized integral intensity of $Gd_2Ti_2O_7$ with different Er concentrations changes with temperature.

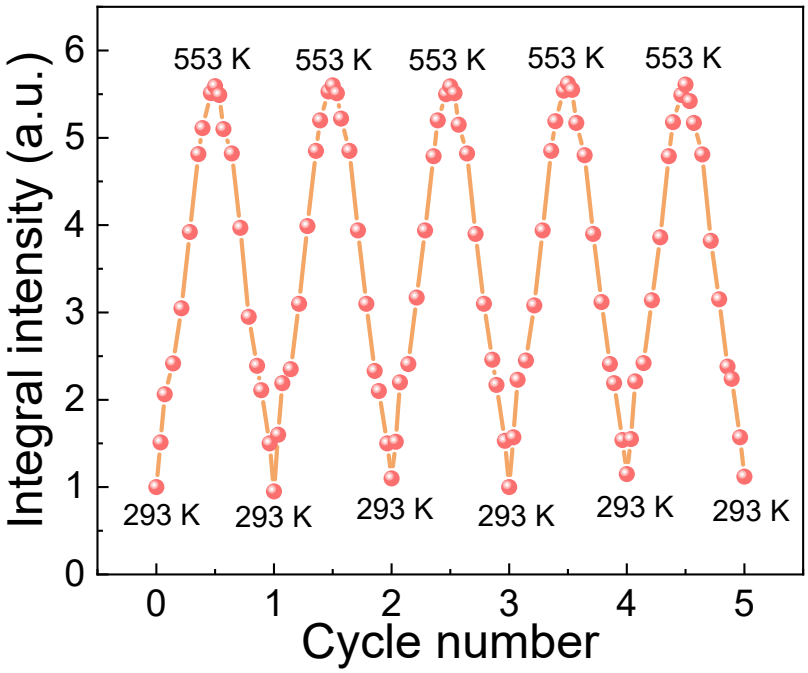

Figure S3. Reversibility of the temperature dependent integral UC emission intensity variations of the $Gd_2Ti_2O_7$: 20Yb/4Er.

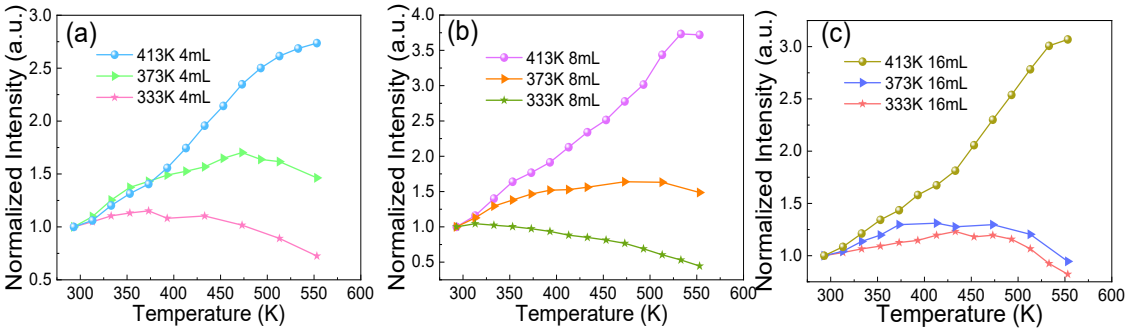

Figure S4. When the amount of ethanol in the precursor solution is 4ml (a), 8ml (b) and 16ml (c) respectively, the normalized integral luminescence intensity of $Gd_2Ti_2O_7$ obtained by evaporating ethanol at different temperatures changes with temperature

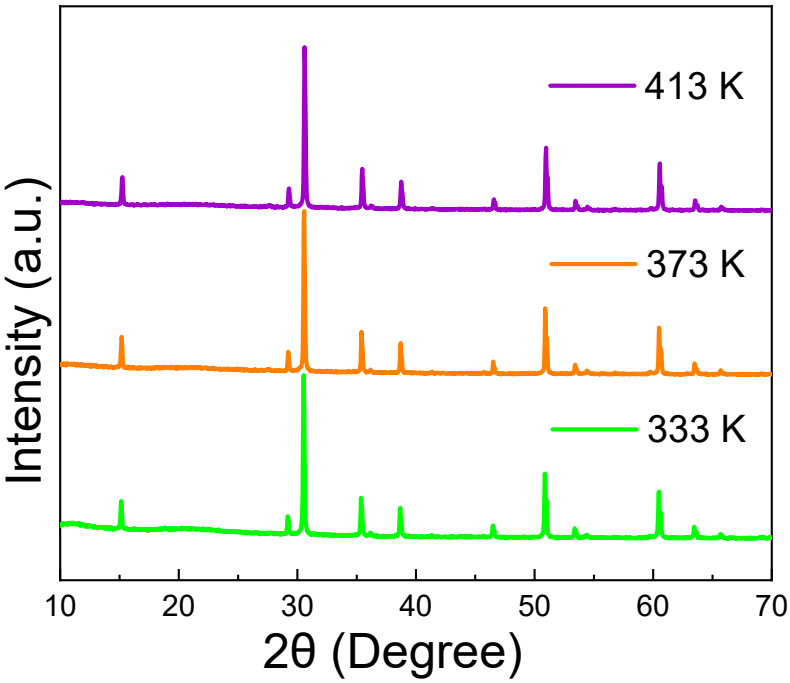

Figure S5. XRD patterns of the $Gd_2Ti_2O_7$: 20Yb/2Er NCs prepared at different evaporating temperature.

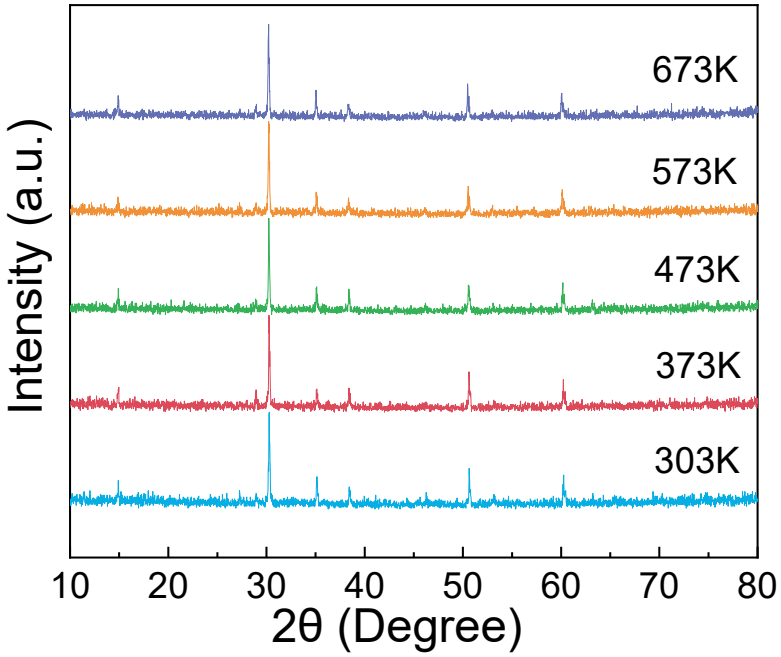

Figure S6. Temperature-dependent XRD patterns of the $Gd_2Ti_2O_7$: 20Yb/2Er NCs

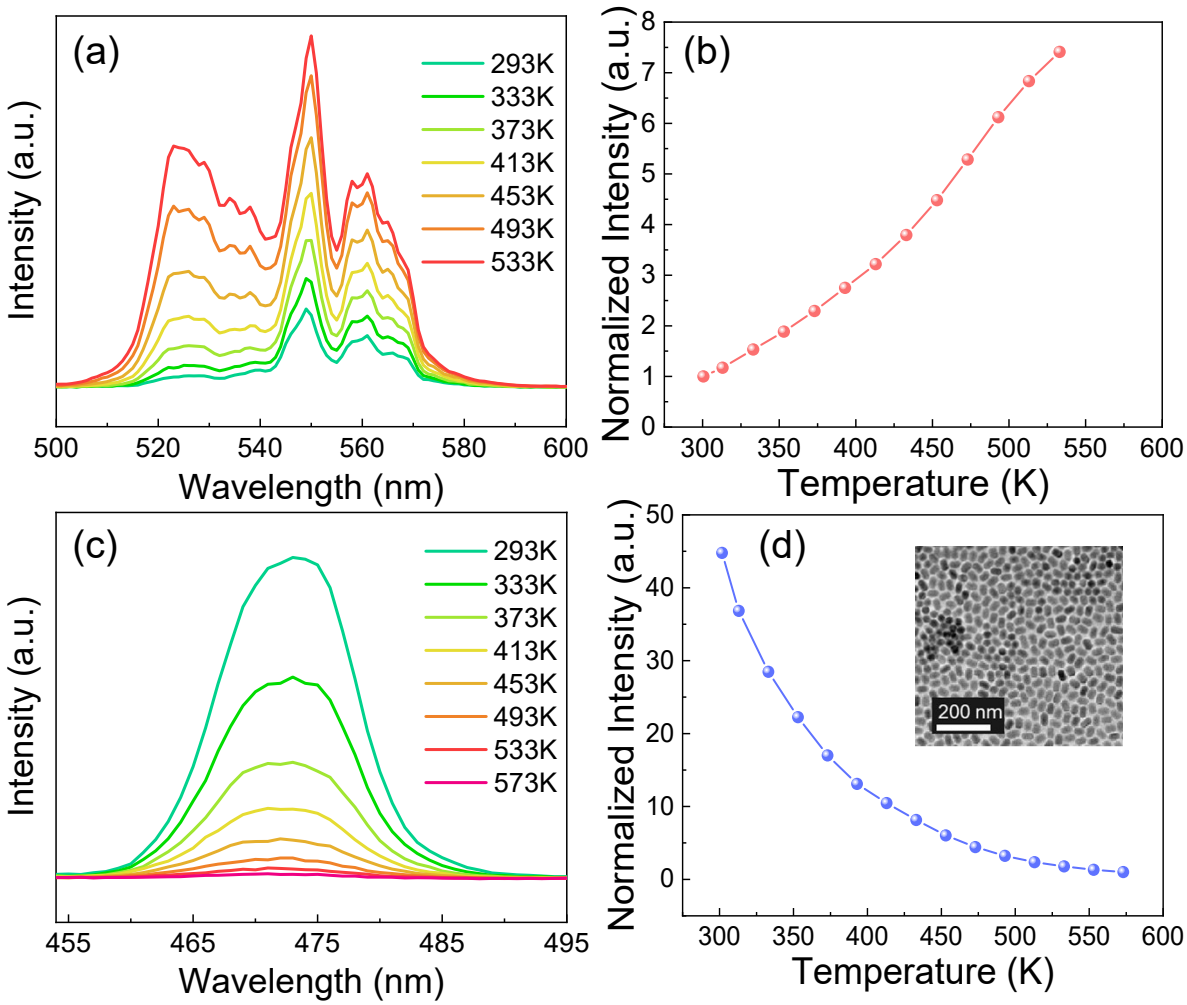

Figure S7. Temperature-dependent green UC emission spectra (a) and variation of normalized integral intensity (b) of the $Gd_2Ti_2O_7$: 30Yb/4Er under the excitation of a 980 nm laser. Temperature-dependent blue UC emission spectra (c) and variation of normalized integral intensity (d) of $NaGdF_4$: 49Yb/1Tm@$NaYF_4$ under the excitation of a 980 nm laser.

Materials	Temperature range (K)	S_a-max(K^{-1})	S_r-max(%K^{-1})	Ref.
$NaBiF_4$:Yb^{3+},Er^{3+}	303-483	0.0057	1.24	S1
Gd_2ZnTiO_6	313-473	0.0218	/	S2
$NaYF_4$:Yb^{3+},Tm^{3+}@$NaYF_4$: 1Pr^{3+}	350-510	/	1.53	S3
$SrAl_2Si_2O_8$:Ce^{3+},Tb^{3+}	293-520	0.034	2.24	S4
$CaSc_2O_4$:Pr^{3+}	275-490	/	2.49	S5
$NaBaSc(BO_3)_2$:Ce^{3+},Mn^{2+}	298-473	/	3.16	S6
$LaPO_4$:Yb^{3+}, Nd^{3+}	280-490	0.074	3.51	S7
$CaNb_2O_6$:Bi^{3+},Eu^{3+}	298-523	0.122	3.793	S8
$GdNbO_4$:Bi^{3+},Eu^{3+}	303-523	0.037	3.81	S9
$LiSr_4(BO_3)_3$:Ce^{3+},Eu^{2+}	293-473	0.057	4.017	S10
$Lu_3Al_5O_{12}$:Ce^{3+},Mn^{4+}	100-350	/	4.37	S11
Li_2TiO_3:Mn^{4+} and Y_2O_3:Dy^{3+}	273-373	0.0263	4.43	S12
Y_2O_3:Ho^{3+} and Mg_2TiO_4:Mn^{4+}	303-373	/	4.60	S13
$Y_3Al_5O_{12}$:Eu^{3+},Mn^{4+}	293-393	0.444	4.81	S14
LaF_3:Er^{3+},Yb^{3+}@LaF_3:Yb^{3+}, Tm^{3+}	293-323	/	5.00	S15
$LiTaO_3$:Ti^{4+},Eu^{3+}	303-443	0.397	5.425	S16
β-$NaYF_4$:Yb^{3+},Ln^{3+} and $NaGdF_4$:Yb^{3+},Ln^{3+}@$NaYF_4$	287-403	/	5.88	S17
Na[$GdSiO_4$]]·xNaOH:Eu^{3+}, Tb^{3+}	0-400	/	6.2	S18
$LaPO_4$:Nd^{3+}	303-573	/	7.19	S19
$Li_5Zn_8Al_5Ge_9O_{36}$:Mn^{2+}	303-383	0.476	8.489	S20
$Gd_2Ti_2O_7$: Yb^{3+},Er^{3+} and $NaGdF_4$: Yb^{3+},Tm^{3+}@$NaYF_4$	293-533	0.65	8.73	This work
Sr_2GeO_4:Pr^{3+}	17-600	/	9.00	S21
$NaYF_4$:Yb^{3+},Er^{3+} and $Yb_2W_3O_{12}$:Nd^{3+}	313-553	3.695	15.3	S22
$NaYF_4$:Yb^{3+},Er^{3+} and $Yb_2W_3O_{12}$:Tm^{3+}	313-553	19.71	23.84	S22

Table S1. Comparison of temperature sensitivities of different reported ratiometric thermometers.

REFERENCES

[1] Du, P.; Luo, L.; Huang, X.; Yu, J. Ultrafast Synthesis of Bifunctional Er^{3+}/Yb^{3+}-codoped $NaBiF_4$ Upconverting Nanoparticles for Nanothermometer and Optical Heater. *J. Colloid Interface Sci*. **2018**, *514*, 172-181.

[2] Wu, Y.; Xu, S.; Xiao, Z.; Lai, F.; Huang, J.; Fu, J.; Ye, X.; You, W. A Universal Strategy to Enhance The Absolute Sensitivity for Temperature Detection in Bright Er^{3+}/Yb^{3+} Doped Double Perovskite Gd_2ZnTiO_6 Phosphors. *Mater. Chem. Front.* **2020**, *4*, 1182-1191.

[3] Zhou, S.; Jiang, G.; Li, X.; Jiang, S.; Wei, X.; Chen, Y.; Yin, M.; Duan, C. Strategy for Thermometry Via Tm^{3+}-Doped $NaYF_4$ Core-shell Nanoparticles. *Opt. Lett*. 2014, *39*, 6687-6690.

[4] Dai,W.; Hu, J.; Liu, G.; Xu, S.; Huang, K.; Zhou, J.; Xu, M. Thermometer of stable $SrAl_2Si_2O_8$: Ce^{3+}, Tb^{3+} based on synergistic luminescence. *Chinese J. Lumin.* **2020**. *217*, 116807.

[5] Wang, S.; Ma, S.; Zhang, G.; Ye, Z.; Cheng, X. High-Performance Pr^{3+}-Doped Scandate Optical Thermometry: 200 K of Sensing Range with Relative Temperature Sensitivity above 2%.K^{-1}. *ACS Appl. Mater. Interfaces*. **2019**, *11*, 42330-42338.

[6] Geng, W.; Zhou, X.; Ding, J.; Wang, Y. Density-functional theory calculations, luminescence properties and fluorescence ratiometric thermo-sensitivity for a novel borate based red phosphor: $NaBaSc(BO_3)(2):Ce^{3+},Mn^{2+}$. *J. Mater. Chem. C*. **2019**, *7*, 1982-1990.

[7] Suo, H.; Zhao, X.; Zhang, Z.; Guo, C. Ultra-sensitive Optical Nano-thermometer $LaPO_4$: Yb^{3+}/Nd^{3+} based on Thermo-enhanced NIR-to-NIR Emissions. *Chem. Eng. J.* **2020**, *389*, 124506.

[8] Zhang, H.; Yang, H.; Li, G.; Liu, S.; Li, H.; Gong, Y.; Liang, Y.; Chen, Y. Enhancing Thermometric Performance via Improving Indicator Signal in Bi^{3+}-doped $CaNb_2O_6:Ln^{3+}$ (Ln = Eu/Sm/Dy/Tb) Phosphors. *Chem. Eng. J.* **2020**, *396*, 125251.

[9] Xue, J.; Noh, H.; Choi, B.; Park, S.; Kim, J.; Jeong, J.; Du, P. Dual-functional of non-contact thermometry and field emission displays via efficient Bi^{3+} -> Eu^{3+} energy transfer in emitting-color tunable $GdNbO_4$ phosphors. *Chem. Eng. J.* **2019**, *11*, 8864-8869.

[10] Li, C.; Chen, B.; Deng, D.; Wu, M.; Yu, H.; Li, H.; Shen, C.; Wang, L.; Xu, S. Ratiometric Optical Thermometer with High-sensitive Temperature Sensing based on Synergetic Luminescence of Ce^{3+}-Eu^{2+} in $LiSr_4(BO_3)_3$ phosphors. *J. Alloys Compd*. **2020**, *838*, 155675.

[11] Chen, Y.; He, J.; Zhang, X.; Rong, M.; Xia, Z.; Wang, J.; Liu, Z. Dual-mode Optical Thermometry Design in $Lu_3Al_5O_{12}$:Ce^{3+}/Mn^{4+} Phosphor. *Inorg. Chem.* **2020**, *59*, 1383- 1392.

[12] Xie, C.; Wang, P.; Lin, Y.; Wei, X.; Yin, M.; Chen, Y. Temperature-dependent Luminescence of a Phosphor Mixture of Li_2TiO_3: Mn^{4+} and Y_2O_3: Dy^{3+} for Dual-mode Optical Thermometry. J. *Alloys Compd.* **2020**, *821*, 153467.

[13] Sekulic, M.; Dordevic, V.; Ristic, Z.; Medic, M.; Dramicanin, M. Highly Sensitive Dual Self‐Referencing Temperature Readout from the Mn^{4+}/Ho^{3+} Binary Luminescence Thermometry Probe. *Adv. Opt. Mater*. **2018,** *6*, 1800552.

[14] Chen, D.; Liu, S.; Zhou, Y.; Wan, Z.; Huang, P.; Ji, Z. Dual-activator Luminescence of RE/TM:$Y_3Al_5O_{12}$ (RE = Eu^{3+}, Tb^{3+}, Dy^{3+}; TM = Mn^{4+}, Cr^{3+}) Phosphors for Self- referencing Optical Thermometry. *J. Mater. Chem. C*. **2016**, *4*, 9044-9051.

[15] Ximendes, E.; Rocha, U.; Sales, T.; Fernandez, N.; Sanz-Rodriguez, F.; Martin, I.;Jacinto, C.; Jaque, D. In Vivo Subcutaneous Thermal Video Recording by Supersensitive Infrared Nanothermometers. *Adv. Funct. Mater*. **2017**, *27,* 1702249.

[16] Wang, C.; Jin, Y.; Yuan, L.; Wu, H.; Ju, G.; Li, Z.; Liu, D.; Lv, Y.; Chen, L.; Hu, Y. A Spatial/Temporal Dual-mode Optical Thermometry Platform based on Synergetic Luminescence of Ti^{4+}-Eu^{3+} Embedded Flexible 3D Micro-rod Arrays:

High-sensitive Temperature Sensing and Multi-dimensional High-level Secure Anti-counterfeiting. *Chem. Eng. J.* **2019**, *374*, 992-1004.

[17] Martinez, E.; Brites, C.; Carlos, L.; Garcia-Flores, A.; Urbano, R.; Rettori, C. Electrochromic Switch Devices Mixing Small - and Large - Sized Upconverting Nanocrystals. *Adv. Funct. Mater*. **2019**, *29*, 1807758.

[18] Ananias, D.; Mongis, C.; Carlos, L.; Rocha, J. Cryogenic Luminescent Ratiometric Thermometers Based on Tetragonal $Na[LnSiO_4] \cdot xNaOH$ (Ln = Gd, Tb, Eu; x ≈ 0.2). *Eur. J. Inorg. Chem*. **2020**, *19*, 1852-1859.

[19] Trejgis, K.; Maciejewska, K.; Bednarkiewicz, A.; Marciniak, L. Near-Infrared-to-Near- Infrared Excited-State Absorption in $LaPO_4:Nd^{3+}$ Nanoparticles for Luminescent Nanothermometry. *ACS Appl. Nano Mater*. **2020**, *3*, 4818-4825.

[20] Wang, Q.; Liao, M.; Mu, Z.;Zhang, X.;Dong, H.; Liang, Z.; Luo, J.; Yang, Y.; Wu, F. Ratiometric Optical Thermometer with High Sensitivity Based on Site-Selective Occupancy of Mn^{2+} Ions in $Li_5Zn_8Al_5Ge_9O_{36}$ under Controllable Synthesis Atmosphere. *J. Phys. Chem. C*. **2019**, *124*, 886-895.

[21] Brites, C.; Fiaczyk, K.; Ramalho, J.; Sojka, M.; Carlos, L.; Zych, E. Widening the Temperature Range of Luminescent Thermometers through the Intra - and Interconfigurational Transitions of Pr^{3+}. *Adv. Opt. Mater*. **2018**, *6*, 1701318.

[22] Wang, Y.; Lei, L.; Ye, R.; Jia, G.; Hua, Y.; Deng, D.; Xu, S.; Integrating Positive and Negative Thermal Quenching Effect for Ultrasensitive Ratiometric Temperature Sensing and Anti-counterfeiting. *Acs Appl Mater Inter*. **2021**, *13*, 23951-23959.